



# Low sensitivity of three terrestrial biosphere models to soil texture over the South-American tropics

Félicien Meunier<sup>1</sup>, Wim Verbruggen<sup>1,2</sup>, Hans Verbeeck<sup>1</sup>, Marc Peaucelle<sup>1,3</sup>

<sup>1</sup>Computational and Applied Vegetation Ecology, Department of Environment, Ghent University, Ghent, 9000, Belgium

<sup>2</sup>Department of Geosciences and Natural Resource Management, University of Copenhagen, Copenhagen, 1350, Denmark

<sup>3</sup>INRAE, Université de Bordeaux, UMR 1391 ISPA, 33140 Villenave-d'Ornon, France

Correspondence to: Félicien Meunier (Felicien.Meunier@ugent.be)

**Abstract.** Drought stress is an increasing threat for vegetation in tropical regions, especially in the context of human-induced increase of drought frequency and severity, as observed over South American forests. Drought stress is induced when a plant's water demand is not met with its water supply through root water uptake. The latter depends on root and soil properties, including soil texture (i.e. the soil clay and sand fractions) that determines the soil water availability and its hydraulic properties. Soil clay content was shown to be responsible for a significant fraction of the spatial variability in forest structure and productivity. Yet, large uncertainties remain for soil textural properties at the regional level and it is currently unclear how those uncertainties propagate into the outputs of Terrestrial Biosphere Models (TBMs) that are used to predict the response of vegetation ecosystems to future climate change scenarios. In this study, we evaluated the heterogeneity in soil textural properties from the global SoilGrids250m product, and we then assessed the sensitivity of the carbon cycle of tree TBMs (namely ORCHIDEEv2.2, ED2, and LPJ-GUESS) to the variability in soil textural properties at the regional level over the South-American tropics using model default pedotransfer functions. When the SoilGrids product was aggregated from its finest (250m) to a coarser spatial resolution typical of TBM simulations (0.5°), the intra-gridcell variability in soil texture rapidly increased to reach an order of magnitude similar to the inter-gridcell variability. All explored model outputs of each TBM, including gross primary productivity, aboveground biomass, soil carbon content and drought stress, were shown to be insensitive to soil texture changes, except for a limited region characterised by low water-availability in ORCHIDEEv2.2 and ED2. We argue that generic pedotransfer and simple drought stress functions, as currently implemented in TBMs, should be reconsidered to better capture the role of soil texture and its coupling to plant processes, which will be critical to properly account for future increasing drought stress conditions in tropical regions.

## Keywords

Soil texture - Terrestrial biosphere model - Pedotransfer functions - Model sensitivity - Drought stress - South-American tropics



## 1 Introduction

30 Over the last three decades, the Amazon tropical forest has been facing an increase in severity and length of drought events  
(Spinoni et al. 2014), a trend which is projected to continue by the end of the century (Duffy et al. 2015). Observations and  
manipulative field experiments have revealed a clear sensitivity of the Amazon forest to severe drought, potentially leading to  
large-scale increase in tree mortality and decrease in forest productivity through reduced photosynthesis (Nepstad et al. 2007;  
35 Phillips et al. 2009; Gatti et al. 2014; Doughty et al. 2015; Corlett 2016; Feldpausch et al. 2016). Increasing tree mortality in  
the Amazon is thought to be induced by soil moisture deficit (low water supply) combined with low air humidity and high air  
temperature (high water demand), which combined leads to hydraulic failure in trees (Rowland et al. 2015). An increased  
vulnerability of the Amazon forest to drought stress will have large impacts on the regional and global carbon, nutrient and  
water cycles as well as the coupled climate system, and has been proposed as one of the factors involved in the observed  
40 decline of the Amazon carbon sink strength (Brienen et al. 2015; Maeda et al. 2015; O'Connell, Ruan, and Silver 2018; Hubau  
et al. 2020).

Soil water availability is intimately related to soil texture. By modulating the retention and accessibility of water (and nutrients)  
to the trees (Silver et al. 2000; Laurance et al. 1999), soil texture, and especially the clay fraction, shapes forest structure and  
function and its spatio-temporal dynamics. At the regional level, clay and nutrient gradients were shown to explain a substantial  
part of the variability in forest biomass, soil carbon pools and forest productivity across the Amazon basin (Laurance et al.  
45 1999; Aragão et al. 2009; Jiménez et al. 2014). The intensity of the dry season and the availability of nutrients (e.g. phosphorus)  
affect species distribution (Condit et al. 2013; Jirka et al. 2007), while soil moisture gradients have also been shown to affect  
plant traits and leaf area index (Fyllas et al. 2009; Flack-Prain et al. 2021). Furthermore, by affecting canopy conductance and  
hence carbon assimilation, soil moisture directly impacts the dynamics of water and carbon fluxes at the tree level (Harris et  
al. 2004).

50 In order to study the resilience of the Amazon forest to future drought, Terrestrial Biosphere Models (TBM) are key tools that  
integrate eco-physiological processes at different spatio-temporal scales and the response of ecosystems to environmental  
changes. In most TBMs, water availability directly affects carbon assimilation through so-called drought stress functions that  
modulate leaf stomatal conductance. Joetzjer et al. (2014) showed that the amplitude and timing of plant response to moisture  
deficit was highly sensitive to these unconstrained functions, which prevented the accurate representation of the impact of  
55 drought over the Amazon rainforest. Consequently, current TBMs are unable to simulate the spatial variability of forest  
productivity and biomass over the Amazon (Johnson et al. 2016). Drought-stress response parameterization and sensitivity  
were also shown to affect the coupling strength between the land surface and the atmospheric boundary layer and thus the  
performance of coupled climate models (Combe et al. 2016). To better capture the drought stress effect on vegetation,  
unprecedented efforts are being made in the community to improve the representation of plant hydraulics in TBMs (e.g.  
60 Christoffersen et al. 2016; Xu et al. 2016; Mencuccini, Manzoni, and Christoffersen 2019). However, less effort has been spent



on enhancing the representation of the soil and its effect in TBMs, despite its key role in drought stress (Carminati and Javaux 2020).

In TBMs, soil moisture is determined by soil hydrology submodels which typically rely on soil textural information and pedotransfer functions. TBMs use a rather limited number of pedotransfer functions while soil texture inputs often resume to  
65 a few products with different spatial resolutions (horizontally and vertically). The main products used for regional and global simulations are the FAO/UNESCO soil map of the world (Batjes 1997), the Harmonized World Soil Database (Nachtergaele et al. 2008) and the more recent SoilGrids250m products (Hengl et al. 2017; Poggio et al. 2021). Those gridded soil maps are not independent from one another, and often aggregated at lower spatial resolution to match other model forcings (e.g. meteorological drivers) which results in average soil properties that neglect inter- and intra-gridcell heterogeneity.

70 To date, the existing evaluations of TBMs response to soil properties mainly focused on hydrology and water fluxes. These analyses tend to show a lack of sensitivity of TBMs to soil texture and composition. For instance, Li et al. (2012) showed that the performance of CABLE remained insensitive to soil water dynamics parameters across three contrasting sites even after improving critical processes related to root functioning. In line with these results, Tafasca et al. (2020) investigated the impact of soil texture on soil water fluxes and storage at different scales with ORCHIDEE, as part of the Land Surface, Snow and Soil  
75 moisture Model Intercomparison Project (LS3MIP; van den Hurk et al. 2016). They showed that, while the model exhibits realistic behaviours at the local scale, it is weakly sensitive to the choice of soil texture maps at the global scale. The effect of soil representation on vegetation and carbon has been sporadically assessed in the literature. By applying the Ecosystem Demography model (ED2) over the Amazon rainforest, Longo et al. (2018) showed different sensitivities of the aboveground biomass to soil texture depending on the rainfall regimes at two contrasting sites. While this study suggests that soil hydraulic  
80 properties mediate the Amazon ecosystem response to rainfall regimes, the authors highlighted that the current parameterization of the model does not account for the diversity in soil structure and is limited for representing certain configurations such as clay-rich soils.

Since soil is a major carbon pool and a key driver of water and nutrient availability for plants, we should expect a large model sensitivity to soil properties, which should propagate into the simulated vegetation and the ecosystem biogeochemical cycles.  
85 This assumption especially applies in a tropical region like South-America that frequently suffers from drought and is characterised by heavily weathered and poor soils. To test this assumption, we explored the sensitivity of the vegetation carbon dynamics to soil texture in three state-of-the-art TBMs, representative of the main classes of commonly used TBMs: LPJ-GUESS, ED2 and ORCHIDEE v2.2. Model sensitivity to soil texture was assessed based on the inter- and intra-gridcell variability in clay content as quantified from the SoilGrid250m database. For each simulation, we present the sensitivity of  
90 soil carbon pools, gross primary productivity (GPP) and aboveground biomass resulting from the different soil configurations, for both the conditions after the model spin-up and the historical simulation spanning the 1860-2016 period. Results of the different simulations for the three models are compared between one another and with existing observation products to assess



model robustness. We finally discuss the main findings in the light of implemented mechanisms and propose future development to improve the representation of the soils and drought stress in TBMs.



## 95 2 Material and Methods

In this study, we explored the sensitivity to soil texture of three state-of-the-art TBMs which occupy different positions along the vegetation representation abstraction continuum that varies from individually-based gap models to area-based big-leaf models. These TBMs, namely LPJ-GUESS, ED2, and ORCHIDEE v2.2, are briefly described in the next three subsections while a more detailed list of parameters, pedotransfer functions, and description of the impact of drought stress on plant productivity for each model can be found in supplementary section 1.

### 2.1 Vegetation models

#### 2.1.1 LPJ-GUESS

The LPJ-GUESS (Lund-Potsdam-Jena General Ecosystem Simulator) model is a process-based dynamic vegetation model which can simulate the global vegetation distribution with its associated carbon, nitrogen and water cycles (Smith, Prentice, and Sykes 2001; Smith et al. 2014). The model has three possible modes of representing vegetation. Population mode is inherited from the LPJ model (Sitch et al. 2003), while individual and cohort mode correspond to the vegetation representation of the GUESS model (Smith, Prentice, and Sykes 2001). For this study, the model was run in cohort mode. Cohorts represent the properties of the average individuals belonging to an age class of a given PFT. However, for herbaceous PFTs the LPJ-GUESS model simulates only one average individual per patch. The coarsest spatial level in this model is the gridcell, for which soil texture, meteorological drivers and nitrogen deposition should be provided. Different stands will each occupy a fraction of a given gridcell, representing different land cover and management types (e.g. natural vegetation, cropland, managed forests, etc.). Each stand contains one (population mode) or multiple (cohort and individual mode) replicate patches. The latter allows the model to account for heterogeneity in age distribution of the vegetation, due to stochastic differences in population dynamics. Within each patch, the different cohorts will grow and compete for light, water and soil nitrogen.

Soil hydrology is represented by a multi-layer bucket model, where water can percolate between the different soil layers and drains at the bottom (Gerten et al. 2004). Soil depth is hard-coded to 1.5 m and subdivided into 15 layers of 10 cm thickness each. Soil moisture in the top two layers (20 cm) is available for surface evaporation. Only two larger percolation layers are defined: excess water from the top (50 cm) layers will percolate into the bottom (100 cm) layers, where it is distributed between the layers depending on their water capacity. Soil hydraulic properties are derived from pedotransfer functions that require sand and clay contents for each gridcell (Cosby et al. 1984; I. C. Prentice et al. 1992; Haxeltine and Prentice 1996). These are assumed to remain constant over the complete soil column. Soil water content is given as a fraction (0-1) of the available water capacity, which is in turn defined as the difference between the volumetric water content at field capacity and wilting point. Plant drought stress is expressed by the ratio between water supply and atmospheric water demand. If water supply is smaller than water demand, the PFT will be drought-stressed and canopy conductance will be reduced. Water supply is calculated as the product of a PFT-specific daily maximum transpiration rate ( $e_{\max}$ ), daily maximum root water uptake and a factor which



represents the leaf phenological status as a fraction of the potential leaf cover. Daily maximum root water uptake is given as a function of the fractional root distribution and plant-available water content, summed over all soil layers. In the standard LPJ-GUESS parameterization, this function is simply the product of both factors, further scaled by the total foliar projective cover in order to account for spatial overlap between cohorts.

### 130 2.1.2 ED2

ED2 (Ecosystem Demography model, version 2) is a cohort-based vegetation model that simulates the energy, water, and carbon cycles of terrestrial ecosystems while accounting for their horizontal and vertical heterogeneities (Medvigy et al. 2009). The model was designed to be compatible with multiple configurations: it can be run as a stand-alone TBM over a single location, over a regional grid, or coupled with an atmospheric model distributed regionally (Knox et al. 2015). In ED2, the  
135 terrestrial ecosystems are represented through a nested hierarchy of structures, which allows scaling up competition for above- and below-ground resources from individual plants to the overall ecosystem (Longo et al. 2019). The coarsest hierarchical level of ED2 is the polygon within which time-varying meteorological forcing above the canopy is assumed uniform. Each polygon is subdivided into one or multiple sites with the aim to represent landscape-scale variations in abiotic properties like soil texture. Within the simulated sites, the horizontal heterogeneities in the ecosystem are simulated through a set of patches  
140 that represent the aggregation of all areas with a similar disturbance history. And finally in each patch, the plant community population is tracked as a collection of plant cohorts, defined by their functional type and size. ED2 has a typical timestep of 10 minutes for the energy and water fluxes but can simulate succession and demography over larger (i.e. century) timescales.

In ED2, plant water availability is determined through a physically-based soil hydrology submodel, which encompasses heat, enthalpy, and water fluxes between different soil layers and the potentially existing temporary surface water. Water flux  
145 between soil layers is based on Darcy's law (Bonan 2008), surface runoff of water is simulated using a simple extinction function while subsurface drainage depends on the bottom boundary condition (e.g. free drainage, zero-flow, saturated water table). In ED2, soil depth, the number of soil layers and layer thickness can be prescribed by the user but in the tropics, the soil is typically discretized into 16 layers along a 8 m depth soil profile with increasing layer thickness from top to bottom (Longo et al. 2019). Most of the soil hydraulic properties in ED2 are derived from the LEAF-3 model (Walko et al. 2000) and  
150 follow the parameterization by Cosby et al. (1984) which is based on the soil volumetric fraction of sand and clay. Soil water retention and hydraulic conductivity curves are respectively based on Clapp and Hornberger (1978) and Brooks and Corey (1964), corrected for partially or completely frozen soil water. Simulated sites are characterised by vertically uniform soil texture and hence hydraulic properties over the entire soil column. Drought stress negatively impacts plant productivity through a non-linear, soil-dependent wilting function, based on the ratio of water demand (plant transpiration) and supply (root water uptake). The latter is proportional to the soil water field capacity minus the soil water at the wilting point, integrated from the  
155 deepest soil layer accessible by plant roots to the soil surface. Rooting depth is related to plant height through an allometric relationship and root biomass is distributed over the soil layers according to their relative thickness.



### 2.1.3 ORCHIDEE v2.2

The process-based gridded vegetation model ORCHIDEE (ORganizing Carbon and Hydrology in Dynamic EcosystEms) is designed to simulate the fluxes of matter and energy, as well as the vegetation dynamics at the regional level (Krinner et al. 2005). ORCHIDEE v2.2 is the land component of the IPSL (Institut Pierre Simon Laplace) climate model developed for the Coupled Model Intercomparison Project Phase 6 (CMIP6), (Eyring et al. 2016). For given vegetation, soil type and climatic conditions, the model simulates physiological processes of an average ecosystem on a half-hourly time step, based on a combination of a dozen Plant Functional Types (PFT) representing the major biomes on Earth.

Drought stress effect on vegetation is simulated through a physically-based soil hydrology scheme and saturation-based Richards equation. The soil is discretized into 11 layers along a 2 m depth profile with increasing layer thickness from the top to the bottom (de Rosnay et al. 2002). Infiltration is processed before soil moisture redistribution while unsaturated values of hydraulic conductivity and diffusivity follow the models of Mualem (1976) and van Genuchten (1980). Soil parameters are set constant for each dominant USDA soil texture class (Carsel and Parrish 1988) provided as input. In ORCHIDEE, the soil texture is uniform over the soil column and only the saturated hydraulic conductivity decreases exponentially with depth to account for soil compaction and bioturbation (d'Orgeval, Polcher, and de Rosnay 2008). To compute infiltration and surface runoff, the model also accounts for horizontal variations in soil hydraulic conductivity (Vereecken et al. 2019). Soil evaporation and transpiration depend on soil moisture and properties, and transpiration is limited by a stomatal resistance which increases when soil moisture drops from field capacity to wilting point. For each PFT, the root density decreases exponentially with depth up to 2 m, thus influencing the drought stress factor on transpiration. The drought stress factor will impact stomatal and mesophyll conductance at the leaf level and hence carbon assimilation. Finally, assimilated carbon is dynamically allocated to several vegetation pools, including the leaves. This will directly influence the seasonality in leaf area index (LAI), which has a feedback on the partitioning between soil evaporation and transpiration, and thus the resulting soil moisture.

## 2.2 Study region and simulation protocol

This study focuses on the South-American tropical region, ranging from 90°W to 30°W in longitude and from 15°N to 20°S in latitude. The spatial resolution of the simulations was set to 1°. For each scenario, long-term spin-up with pre-industrial atmospheric CO<sub>2</sub> concentration from 1860 (287.14 ppm) were performed to each grid cell starting from near bare ground conditions. This was achieved by recycling the initial 10 years of the 6-hourly CRU-NCEP v7 meteorological forcing dataset (Viovy 2018) until soil and vegetation carbon pools reached an equilibrium. No land-use changes were applied to any simulation but a land cover mask representative of the current PFT distribution as derived from the ESA-CCI Land cover map (Poulter et al. 2015) is applied by default to ORCHIDEE simulations. The spin-up runs were continued with historical simulations from 1860 to 2016 for each model using the full CRU-NCEP forcing dataset and varying atmospheric CO<sub>2</sub> concentration according to Friedlingstein et al. (Friedlingstein et al. 2020).



### 2.3 Soil scenarios and model parameterization

190 We performed three regional simulations with each model, using different soil texture maps. These three soil maps represent  
the soil texture corresponding to the average (Mean clay), minimum (Min. clay), and maximum (Max. clay) topsoil clay content  
of each  $1^\circ \times 1^\circ$  grid cell from SoilGrids250m (Poggio et al. 2021), see Figure 1. Soil texture was assumed vertically uniform  
for each model and simulation. For each model, both the soil depth and the number of soil layers were set up according to the  
most default model configurations (Table 1). Similarly, most default model PFT parameterizations were used for each model.  
195 More detail on each model's parameter sets can be found in the aforementioned references describing the three models. In  
ED2, we simulated four competing PFT (grass, early-, mid-, and late-successional tropical trees) similarly to Longo et al.  
(2019) for Amazon regional runs. To facilitate inter-model comparisons, we chose to run multiple ED2 simulations for each  
polygon rather than simulating multiple sites per polygon. For the LPJ-GUESS model we activated all PFTs as for global  
simulations (Sitch et al. 2003; Ahlström et al. 2012), but due to bioclimatic limits only tropical broadleaf evergreen and  
200 raingreen trees as well as  $C_4$  grasses emerged from the simulation with nonzero biomass.

### 2.4 Analyses

To assess the relative importance of the intra-gridcell variability, we aggregated the topsoil clay fraction in SoilGrids from its  
finest (250m) to a much coarser ( $5^\circ$ ) resolution with the R package 'raster'. For each resolution, we compared the grid-level  
average of the clay fraction standard deviation within each gridcell (i.e. the intra-gridcell variability) with the grid-level  
205 standard deviation of the average clay fraction of each gridcell (i.e. the inter-gridcell variability).

All the results from the vegetation model simulations presented below are averages of the ten last years of either the spin-up  
or the historical period (2006-2016) or of the very end of the historical period (2016). We particularly focused on the inter-  
model and inter-scenario comparison of GPP at the ecosystem- and the PFT levels, as well as the resulting plant above-ground  
biomass. For each simulation of each model, we also computed from the model outputs the normalised soil drought stress  
210 index (SDI) whose definition is model-specific (see supplementary section 1) but always normalised between 0 (full stress)  
and 1 (no stress). We related SDI to the ecosystem GPP through quantile regression analyses using the R package 'quantreg'.

The soil textures across the three scenarios were also classified according to the 12 major soil texture categories defined by  
the United States Department of Agriculture (Soil Survey Manual, 2017), using the 'soiltexture' R package (Moeys, 2018),  
which allowed us to quantify soil class frequencies for each soil scenario and to define transition matrix when switching from  
215 one soil textural map to another. All analyses and plots were performed in R version 3.6.3. The corresponding code to generate  
the results and reproduce the figures below is available on Github (<https://github.com/femeunier/SoilSensitivity>) with an  
archived version on Zenodo (10.5281/zenodo.6226622) corresponding to tag v1.





## 2.5 Evaluation datasets

220 We used three different datasets to assess the model robustness and performance under the three soil scenarios. First, we  
compared the spatial distribution of aboveground biomass as simulated by the models with the integrated biomass map of  
Avitabile et al. (2016) over the study region. This biomass map is one of the reference products used by the International  
Model Benchmarking system (ILAMB; Collier et al. 2018) to evaluate TBMs, as for example in the global carbon budget  
exercise (Friedlingstein et al. 2020). Secondly, we contrasted the model outputs of ecosystem GPP with a moderate resolution  
dataset of vegetation gross primary production for the years 2006-2016 driven by satellite data from MODIS (MOD17A2),  
225 see Running et al. (2015). Finally, we differentiated the soil organic carbon stocks produced by each vegetation model and  
derived from local observations upscaled to the globe in SoilGrids.



### 3 Results

#### 3.1 Intra- and inter-gridcell variability in topsoil clay content

230 With the native spatial resolution of the SoilGrids product (250m), we observed a wide distribution in clay content over the South-American tropics ranging from nearly 0% to 74%, with a median around 28% and a standard deviation of 7% (Figure 1A). Such extreme clay content values can also be found within gridcells when using the spatial resolution typically applied in TBMs: in the magnified 1° gridcell (~111 km at the equator) of Figure 1A, clay fraction varied between 0 and 58% with a median and a standard deviation of 23% and 7%, respectively. When SoilGrids was aggregated from its finest to coarser spatial  
235 resolutions, we observed a rapidly increasing intra-gridcell variability in soil texture: over the whole region, the average intra-gridcell variability (i.e. the mean standard deviation) in clay content strongly raised by 4% from 250m to 1°, and kept increasing up to 6% at 5°. At 1° resolution and coarser, the variability within and between gridcells reached similar order of magnitudes (Figure 1B). The three soil scenarios were built on this intra-gridcell variability in soil texture: we generated three soil maps at 1° resolution based on the maximum, average and minimum clay fraction within each gridcell. A clear shift from sandy/silty  
240 soils toward more clayey soils can be observed when moving from the Min. Clay to the Max. Clay scenario (Figure 1C and supplementary Figure S1A). The resulting changes in sand fraction density distributions were less marked, except for the Min. clay scenario (supplementary Figure S1B).

#### 3.2 Models performance in default configuration

In their most default configuration, all three models showed poor performances in capturing the spatial variability in  
245 aboveground biomass (Figure 2), GPP (Figure 3) and soil carbon content (supplementary Figure S1) as estimated from independent products, regardless of the soil scenarios.

The reference aboveground biomass map from Avitabile et al. (2016) shows a bimodal distribution in biomass over the South-American tropics as a reflection of the distribution in forest ( $12.5 \pm 2.7 \text{ kg}_C \text{ m}^{-2}$ ) vs non-forest biomes ( $2.4 \pm 2.3 \text{ kg}_C \text{ m}^{-2}$ , see Figure 2). Both the ORCHIDEE v2.2 and ED2 models reproduced this bimodal distribution (non forest peak at  $3.1 \pm 2.3 \text{ kg}_C \text{ m}^{-2}$  and  $0.7 \pm 1.5 \text{ kg}_C \text{ m}^{-2}$ ; forest peak at  $12.3 \pm 1.8 \text{ kg}_C \text{ m}^{-2}$  and  $17.5 \pm 2.4 \text{ kg}_C \text{ m}^{-2}$ , respectively), but also overestimated the overall aboveground biomass on average ( $8.0$  and  $11.4 \text{ kg}_C \text{ m}^{-2}$  for both models respectively while data average is  $6.7 \text{ kg}_C \text{ m}^{-2}$ ). On the contrary, LPJ-GUESS simulated a unimodal biomass distribution with an overestimated average biomass of  $12.0 \pm 5.5 \text{ kg}_C \text{ m}^{-2}$ . When compared to remote sensing estimates over the 2006-2016 period, ORCHIDEE v2.2 and ED2 overestimated the gross primary productivity with simulated average values of  $2.4 \pm 1.0 \text{ kg}_C \text{ m}^{-2} \text{ yr}^{-1}$  and  $3.3 \pm 1.5 \text{ kg}_C \text{ m}^{-2} \text{ yr}^{-1}$ , respectively,  
255 compared to reference values of  $2.2 \pm 0.3 \text{ kg}_C \text{ m}^{-2} \text{ yr}^{-1}$ . Only LPJ-GUESS simulated similar average values of  $2.2 \pm 0.6 \text{ kg}_C \text{ m}^{-2} \text{ yr}^{-1}$ . Finally, all three models overestimated soil C content compared to the information from the SoilGrid database with LPJ-GUESS, ED2 and ORCHIDEE v2.2 respectively simulating mean values of  $14.8 \pm 6.3 \text{ kg}_C \text{ m}^{-2}$ ,  $10.6 \pm 8.2 \text{ kg}_C \text{ m}^{-2}$ , and  $7.6 \pm 2.9 \text{ kg}_C \text{ m}^{-2}$  for a reference value of  $4.3 \pm 1.7 \text{ kg}_C \text{ m}^{-2}$ . Also the simulated spatial distributions of the soil C content were



260 drastically different from the reference one (Figure S2), regardless of the soil scenario. The relative better performance of the ORCHIDEE model in capturing the spatial variability in vegetation and soil carbon stocks can be partly explained by the use of a land cover map to constrain vegetation type distribution compared to ED2 and LPJ-GUESS for which the PFT distribution is an emergent property of the models.

### 3.3 Model sensitivity to clay content variability

265 Large differences existed between models for the same soil scenario. However, the performance of each model was almost independent of the soil scenario for all investigated products (AGB, GPP, soil C). All three models exhibited a strong correlation between the soil drought stress index (SDI) and the overall ecosystem productivity (Figure 3). Across the three scenarios, we observed that increasing clay content (mean clay fraction of 17%, 28%, and 34% in the Min. clay, Mean clay, and the Max. clay scenario, respectively) slightly increased drought stress (i.e. decreased SDI) by 2.6, 0.7 and 1.5% (change of the drought stress index from the Min. clay to the Max. clay scenario) for ORCHIDEE, ED2 and LPJ-GUESS, respectively.  
270 This increase in simulated drought stress was accompanied by a decrease in productivity for all three models, respectively by 2.7, 1.9 and 3.2%.

Nonetheless, we observed substantial changes in PFT-level GPP simulated for the three scenarios for some gridcells (Figure 4) especially for the ORCHIDEE model, which indicates some shifts in the simulated PFT composition. This situation occurred in about 3% of the gridcells for ED2, 6% of the gridcells for LPJ-GUESS, and 7% for ORCHIDEE when switching from the  
275 Mean clay scenario to the Min. clay or the Max. clay scenario. Yet, these PFT-level shifts in GPP compensate for each other when aggregated at the ecosystem level, resulting in similar total GPP and spatial distributions that remain almost unaffected by shifts in soil composition (Figure 3). Not only the simulated Soil Moisture Index and GPP did not change substantially, but we also observed very limited shifts in soil C content (supplementary Figure S2) and aboveground biomass in response to changes in soil clay content (Figure 2). Between the Min Clay and Max Clay scenarios, we observed a 3.0%, 0.7% and 4.2%  
280 increase in the average simulated aboveground biomass, and a -11.9%, 10.1% and 7.6% change in soil C content, as simulated by ORCHIDEE, ED2 and LPJ-GUESS. All the aforementioned observations also apply to state conditions resulting from the spin-up phase (as exemplified for the AGB spatial distribution at the end of the spin-up for all three models and all three scenarios, see supplementary Figure S3).

We observed some significant impacts of the scenario on the ecosystem GPP (up to a 100% change of ecosystem GPP) for  
285 some of the soil textural class transitions (which represent the frequency of soil class changes when moving from one soil textural map to another), but those transitions were rather rare events and hence limited to a small area of the simulated region (Figure 5). The most frequent transitions were within the same soil class (the diagonal of the soil transition matrix of Figure 5A): those represented 32% of all transitions between the Mean clay and the Min. clay scenarios, and 43% of all transitions between the Mean clay and the Max. clay scenarios) and were almost unaffected by the soil clay content (relative change of ecosystem GPP between -0.6% and 2.1% for all models and scenarios). For both ED2 and ORCHIDEEv2.2, most important  
290



changes occurred over (very) low water-availability regions (Mean Annual Precipitation or MAP < 1000 mm for ED2, MAP < 2000 mm for ORCHIDEE) while the sensitivity to soil texture was independent of the water availability in LPJ-GUESS (Figure 6). Yet, only a small fraction of the water-limited area was concerned by changes of simulated state variables: 20% of the gridcells with MAP < 1000 showed a relative change of the ecosystem GPP larger than 10% in both ED2 and ORCHIDEEv2.2. Moreover, positive and negative shifts balanced one another and hence had a very limited impact on the regional ecosystem productivity (Figures 3 and 6).

Finally, we note that the LPJ-GUESS model crashed for some specific soil textures. Those soil textures occur naturally in the field and were relatively frequent in our simulations, especially in the Min. clay scenario (5.4% of the gridcells). The problem occurred for silty soils with low fractions of both sand (< 12%) and clay (25%). The default pedotransfer functions applied to those specific soil textures led to volumetric water content at field capacity larger than the water content at saturation (see supplementary Figure S4), which caused the model to crash during model initialization for those particular gridcells.



#### 4 Discussion

By selecting the dominant soil texture class, a significant fraction of the soil spatial heterogeneity is omitted in TBMs running at coarse spatial resolution (Figure 1), an effect that has already been documented in Tafasca et al. (2020) who suggested that spatial aggregation statistically enhances medium textures, leading to excessive evapotranspiration and insufficient total runoff. Accounting for subgrid variability in soil texture and moisture through systematic sensitivity analysis, or directly representing this effect in TBMs with models (Qu et al. 2015) could alleviate these uncertainties and improve model performance. Intra-gridcell variability in soil texture might have large impacts on simulating vegetation dynamics, especially in demographic models for which plant competition and access to resources drive ecosystem composition and dynamics (i.e. growth/mortality) (Rowland et al. 2015; Johnson et al. 2016). In addition to the aggregation bias, we also expect substantial biases in simulated ecosystem properties resulting from intrinsic uncertainties from soil products. SoilGrids maps of soil properties are generated using machine learning methods that account for direct soil observations and environmental variables describing vegetation, climate, topography, geology and hydrology. However, the number of soil observations available over the Amazon tropics remains very low (10 or fewer soil textural observations for gridcell of 70,000 km<sup>2</sup> for many gridcells in the studied area), potentially leading to high uncertainties in regional soil properties at fine resolution (Poggio et al. 2021, see in particular supplementary Figure S6).

Regardless of the underlying uncertainties in global soil products, we found that the soil carbon content, the aboveground biomass and the gross primary productivity simulated by all TBMs considered in this study were mostly insensitive to soil texture, except for some limited areas with low water availability in ED2 and ORCHIDEEv2.2. In TBMs, plant functions and soils are coupled by a drought stress function which depends on soil moisture. We suggest that the overall lack of sensitivity that we observed originates from the combination of two main limitations in the current implementation of the hydrology submodel in TBMs: 1) the shifts in soil texture resulting from the spatial variability in soil clay content does not translate into realistic shifts in soil hydraulic properties (see Supplementary Figure S5) and 2) the implemented drought stress functions do not properly capture the effect of changes in soil hydraulic properties on vegetation. Both limitations should be rapidly tackled in order to improve TBM performance (Fisher and Koven 2020) and are briefly discussed below.

Current TBMs are using a limited number of generic, widespread pedotransfer functions, which can be class-based or continuous. However, most of these functions were developed and calibrated decades ago (1984 and 1988, see Table 1) with fewer and less geographically spread calibration data than what is available today. On top of the limited size of the training data (especially for the tropical regions), the main drawback of these pedotransfer functions resides in their inability to capture the variability and non-linearity of many parameters for given soil textural classes. For example in their review, Van Looy et al. (2017) highlighted large differences in saturated hydraulic conductivity within each soil class derived from different data sources and location. As a result, by using generic and global functions, soil parameters in TBMs are substantially different from region-specific observations (Kishné et al. 2017; Van Looy et al. 2017). Such generic, global functions could therefore



335 lead to inaccurate characterisation of the soil properties, as illustrated by the LPJ-GUESS crashes with realistic soil compositions (Supplementary Figure S4). Since no generic functions are able to properly capture soil properties at the global scale (Patil and Singh 2016), intermediate solutions should be implemented in TBMs for a better representation and scaling of soil properties. For example, region-specific pedotransfer functions, regional calibration, ensemble simulations using multiple pedotransfer models or also the combination of regional pedotransfer functions could be used to estimate the uncertainties that soil properties are responsible for (Hodnett and Tomasella 2002; Barros and de Jong van Lier 2014; Medeiros et al. 2014).

340 Soils have a direct, strong role in the response of plants to drought (Carminati and Javaux 2020). All three vegetation models used in our study apply simple drought stress functions that depend on the available water and the water demand (Table 1, and Supplementary section 1). We observed that shifting soil properties from low to high clay content barely affected the simulated soil drought stress despite substantial changes in soil texture and classification (Figures 1, 3 and supplementary Figure S1). Even if the sensitivity to soil texture might be increasing with drought stress (Figure 6) and hence under future climate change

345 scenarios, it confirms that generic drought stress functions are not suitable to capture the impact of changes in plant water availability on plant processes, as suggested from previous studies (Joetzjer et al. 2014; Combe et al. 2016) and argues for a better representation of root-soil coupling in TBMs. To reproduce the annual pattern of net ecosystem exchange of carbon over the Amazon with the Simple Biosphere Model (SiB3), Baker et al. (2008) demonstrated the importance of combining multiple mechanisms, not only related to soil water distribution but also on root dynamic schemes. Indeed, the Amazon forest was

350 shown to have high GPP during the dry season (Green et al. 2020; Negrón Juárez et al. 2007), and the role of water uptake with deep roots is currently not properly simulated in TBMs, e.g. because of the shallow soils (and hence root systems) that are simulated (Table 1), (Verbeeck et al. 2011). Recent developments in the TBM community have focused on improved plant hydraulics but to a lesser extent to the root-soil interactions (Xu et al. 2016). Recent studies have demonstrated the need for a better representation of root water uptake in drying soils to simulate plant response to drought stress and its impact on biomass.

355 For instance, the new dynamic root scheme (Joetzjer et al., under review) coupled to explicit plant hydraulic processes in ORCHIDEE managed to reproduce observed water and carbon dynamics at the Caxiuanã throughfall exclusion field experiment in eastern Amazonia (Yao et al. 2021). Although they better capture biomass and flux dynamics at the site level, the new implementations of plant hydraulics is empirical and complex, and leads to an increased number of model parameters and hence to a larger required size of field observational data to calibrate it. Such data are not readily available for a large

360 number of sites or a larger area and/or might be difficult to measure, especially in complex ecosystems like tropical forests. The process of model complexification might also result in over-fitted simulations at the site level, mainly focusing on climate factors (e.g. drought) while overlooking the unconstrained soil and root properties. Better estimate of water demands based on eco-evolutionary optimality theories (Prentice et al. 2014), root biomass (Franklin et al. 2012) and soil-root interactions (Lu et al. 2020; Vanderborght et al. 2021) could help bridge the gap between complex and over-parameterized models on the one hand

365 and simple unrealistic model-specific functions on the other.



370

Finally, soil texture and clay content have a direct, strong impact on the distribution and mineralization of carbon and nutrients in soils (e.g. Hassink 1992; Telles et al. 2003; Plante et al. 2006; Zinn et al. 2007). In our simulations, the three TBM could not reproduce SoilGrid soil carbon distribution and showed very low sensitivity to changes in clay content (Supplementary Figure S2) despite long-term spin-up during which we expected large differences between equilibrium states induced by different soil composition. This further highlights the poor representation of soil processes in TBMs and their coupling to vegetation dynamics. As for the relationship between soil hydraulic properties and texture, we argue that current development focusing on soil processes in TBMs (e.g. nutrient mineralization, soil organic carbon, etc.) should systematically assess model sensitivity to soil properties and texture spatial variability.



375 **5 Conclusion**

TBMs are keystones of global carbon and water budgets assessments and past developments strongly focused on representing plant processes and their response to climate. Despite their importance and recent efforts from the TBM community, belowground processes remain overlooked. Here, we showed that 1) subgrid soil heterogeneity in texture is high at the spatial resolution of typical TBM simulations and 2) carbon related processes in TBM are insensitive to soil texture over the South American tropics. These two results suggest a poor representation of the soil-vegetation coupling in TBMs, mainly because of inadequate pedotransfer and soil drought stress functions. To date, the use of generic pedotransfer and drought stress functions is common in TBMs used for carbon and water budget assessments, as well as future projections, which leads to large errors in the model predictions. Appropriately representing soil spatial heterogeneity and soil-plant coupling, such as the non-linearity of soil-root resistance, is a major challenge that needs to be urgently addressed in TBMs to better represent the effect of drought stress on vegetation and reduce carbon budget uncertainties, especially in complex and heterogeneous ecosystems such as tropical forests.





### Data and code availability

390 SoilGrids250m data are available at: <https://soilgrids.org/>. CRUNCEPv7 data are available at:  
<https://rda.ucar.edu/datasets/ds314.3/>. The code used to generate the results, soil scenario and to reproduce the figures of this  
manuscript is available on Github (<https://github.com/femeunier/SoilSensitivity>) with an archived version on Zenodo  
(10.5281/zenodo.6226622) corresponding to tag v1. The code source of the ORCHIDEE v2.2 model is available at:  
[https://forge.ipsl.jussieu.fr/orchidee/browser/branches/ORCHIDEE\\_2\\_2?order=name](https://forge.ipsl.jussieu.fr/orchidee/browser/branches/ORCHIDEE_2_2?order=name), please contact the ORCHIDEE team at  
<https://orchidee.ipsl.fr/contact/> before any intended usage of the model. The code source of the ED2 model is available at:  
395 <https://github.com/EDmodel/ED2>. The code source of the LPJ-GUESS model is available upon request at:  
<https://web.nateko.lu.se/lpj-guess/>.

### Author contributions

All co-authors designed the study. FM ran the ED2 simulations, MP ran the ORCHIDEE v2.2 simulations, and WV ran the  
LPJ-GUESS simulations. FM analysed the model outputs, and FM and MP wrote the first version of the manuscript. All co-  
400 authors critically revised it.

### Competing interests

Hans Verbeek is a member of the editorial board of Geoscientific Model Development.



## Acknowledgements

405 This research was funded by the Fonds Wetenschappelijk Onderzoek (FWO grant n° G018319N). The computational resources  
and services used in this work were provided by the VSC (Flemish Supercomputer Center), funded by the Research Foundation  
- Flanders (FWO) and the Flemish Government – department EWI. ORCHIDEE simulations were performed using HPC  
resources from GENCI-TGCC (Grant A0110106328). During the preparation of this manuscript, F.M. was funded by the FWO  
as a junior postdoc and is thankful to this organisation for its financial support (FWO grant n° 1214720N). W.V. was funded  
410 by the ArboreSens (Dryland woody vegetation sensitivity to soil texture and precipitation variability) dissemination and  
support project (BELSPO STEREO III; Grant no. SR/02/209). M.P. would like to acknowledge the financial support from the  
H2020 Marie Skłodowska-Curie Actions (LEAF-2-TBM grant no. 891369). H.V. acknowledges the support from the European  
Research Council Starting Grant 637643 TREECLIMBERS.



415 **Tables and Figures**

**Tables**

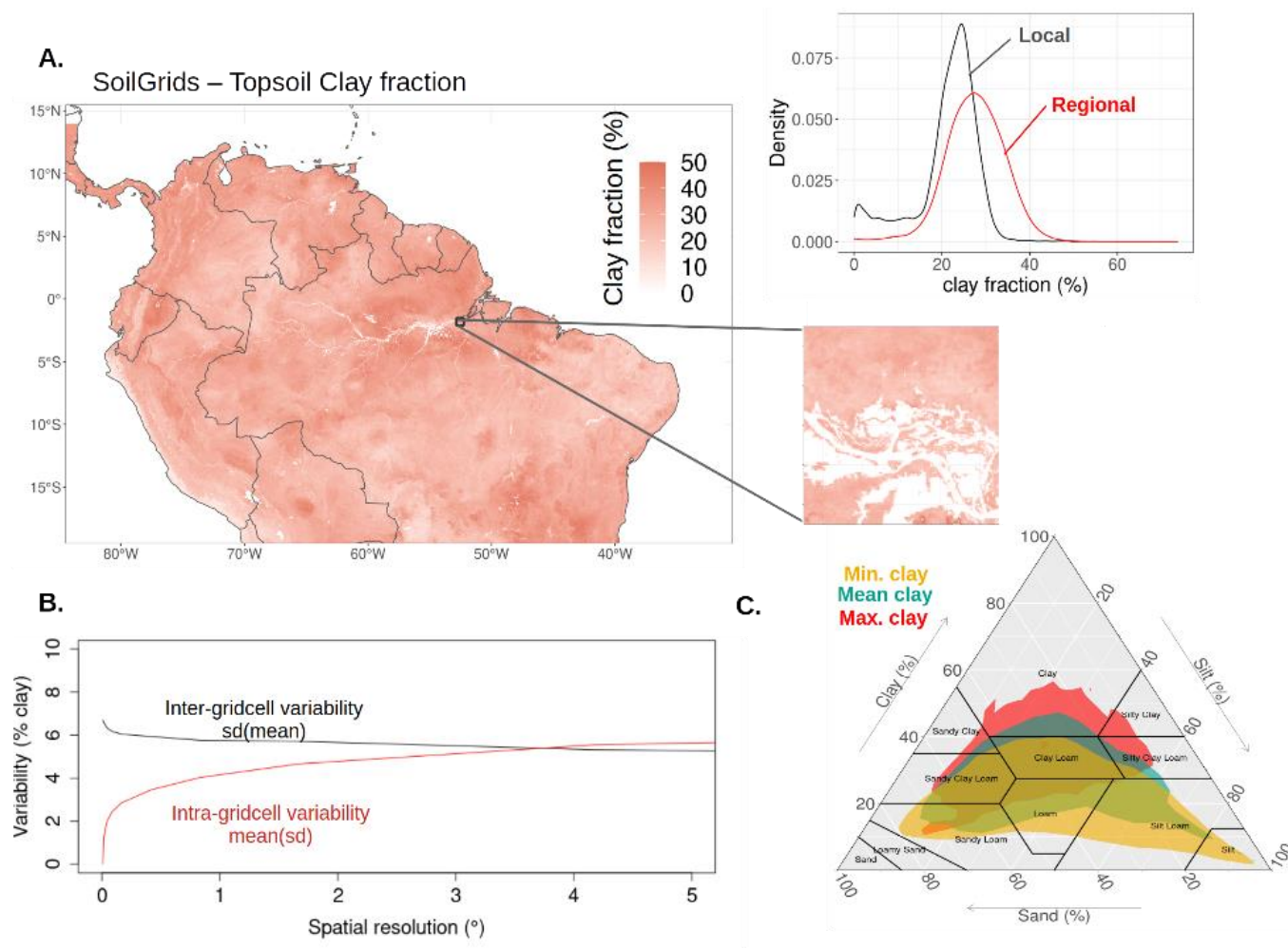
**Table 1: Summary of the representation of soil, roots and soil drought stress for each model in their default version**

Model	Soil depth	Soil texture	Roots	Plant Hydraulics	Drought stress	Impact of drought	Soil pedotransfer functions
<b>LPJ-GUESS</b>	1.5 m	Variable (continuous)	Fractional distribution over each layer, or exponential profile with PFT-dependent decay factor	None (under development)	Non-linear function of water supply and demand	Leaf stomatal conductance	Cosby et al. (1984)
<b>ED2</b>	Variable	Variable (continuous)	No vertical distribution	Optional	Non-linear function of water supply and demand	Leaf stomatal conductance	Cosby et al. (1984)
<b>ORCHIDEE v2.2</b>	2 m	Constant for each USDA class	Exponential profile with a PFT-dependent decay factor	None (under development)	Linear function of wilting point and field capacity	Leaf mesophyll and stomatal conductance	Carsel and Parrish (1988)

420



## Figures



425 **Figure 1: Topsoil (0-5cm) clay fraction spatial distribution as defined by the latest version of SoilGrids with a magnified example of**  
430 **a 1x1° gridcell (A). The Min., Mean, and Max. clay scenarios are those soil types that are characterised respectively by the minimum,**  
**average, and maximum clay fraction content in each gridcell, excluding those without soil textural information (for instance the**  
**rivers as illustrated in the magnified map). In panel A, the density plot reveals the clay fraction distribution at the regional and local**  
**(magnified gridcell) levels. Subplot B shows the difference between the intra-gridcell and the inter-gridcell variability as a function**  
**of the spatial resolution. Subplot C is the resulting soil texture distribution for each scenario, showing a clear shift toward larger**  
**clay contents in the Max. clay scenario.**

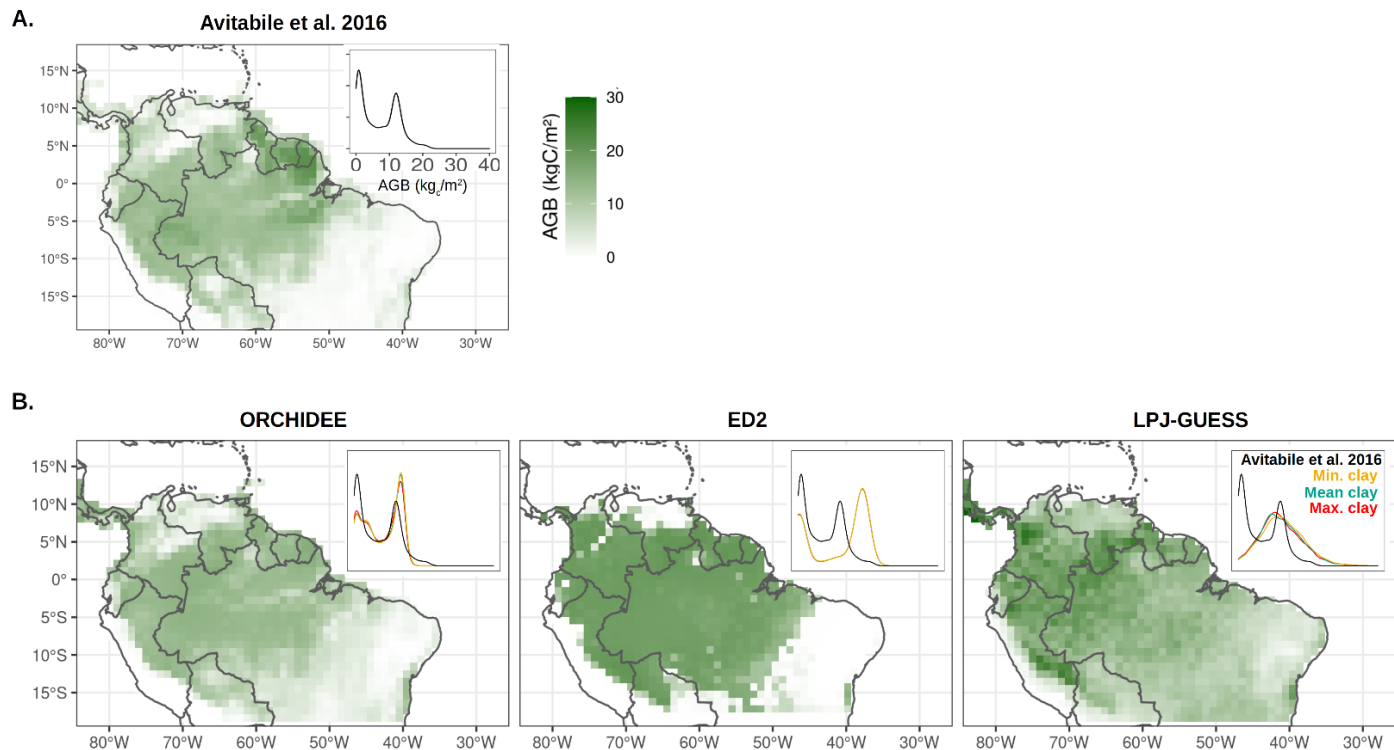
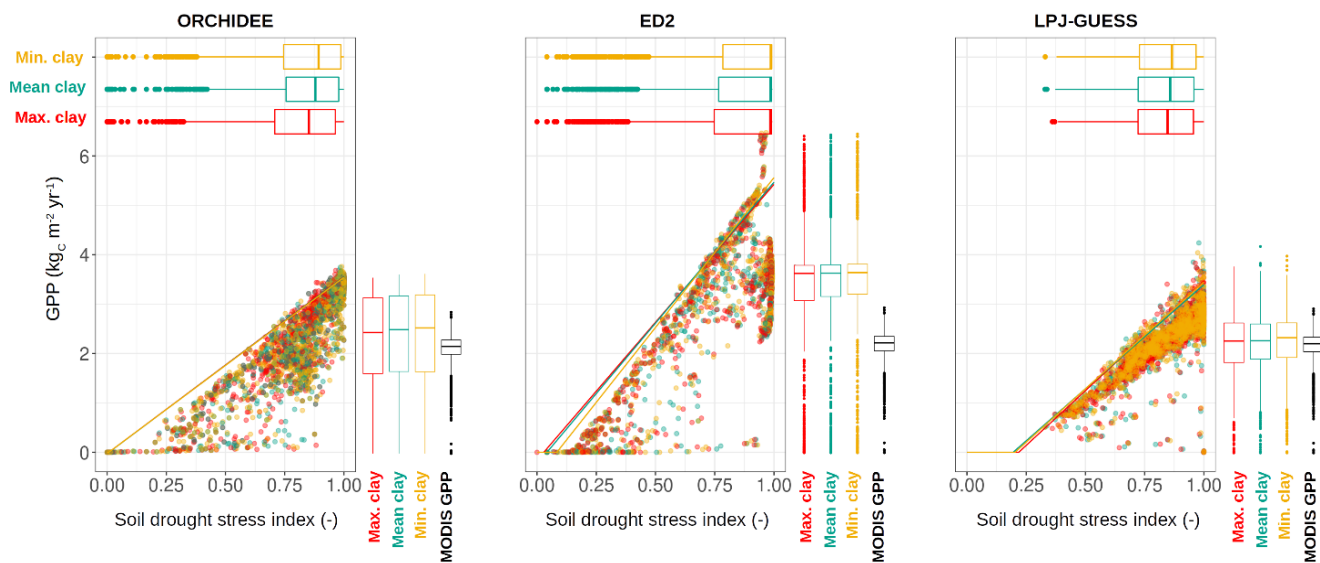
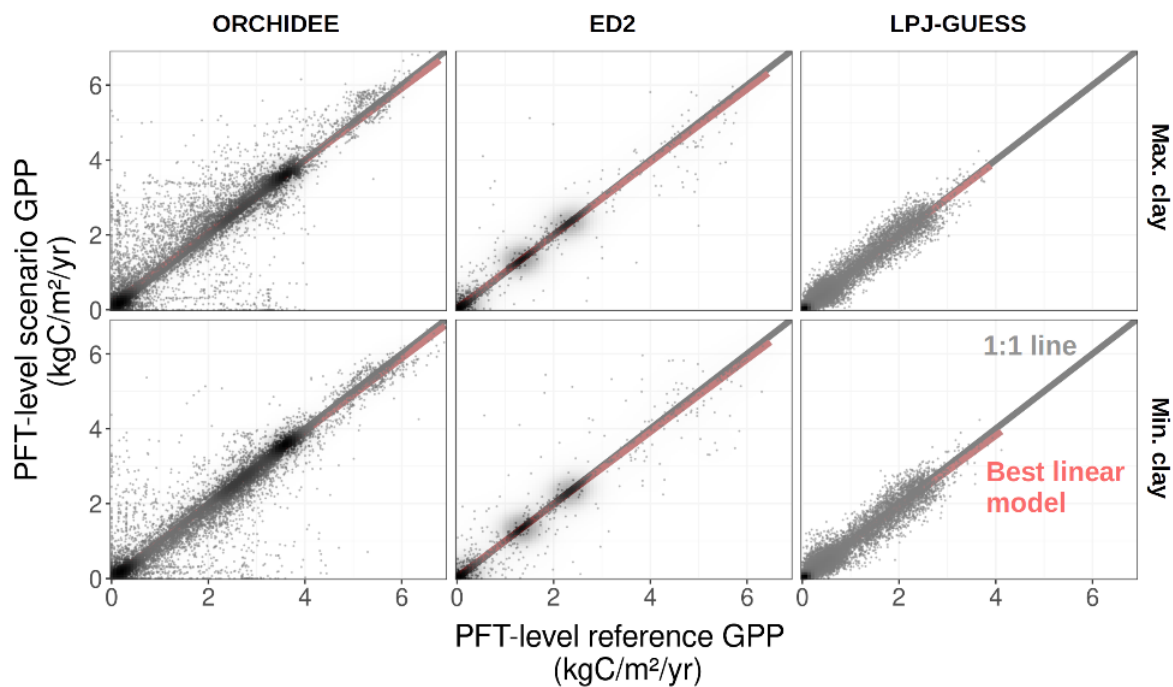


**Figure 2: Above-ground biomass spatial distribution, as generated by Avitabile et al. (2016) (A) or as predicted at the end of the historical period (average over the 2006-2016 period) by the three terrestrial biosphere models used in this study for the Mean clay scenario (B). The upper-right corners in each plot represent the above-ground biomass density distributions over the simulated region for all three scenarios (coloured lines) and the observations (black). Note that the land cover was prescribed in the ORCHIDEE model, while it was an emergent property of the ED2 and LPJ-GUESS models.**

435

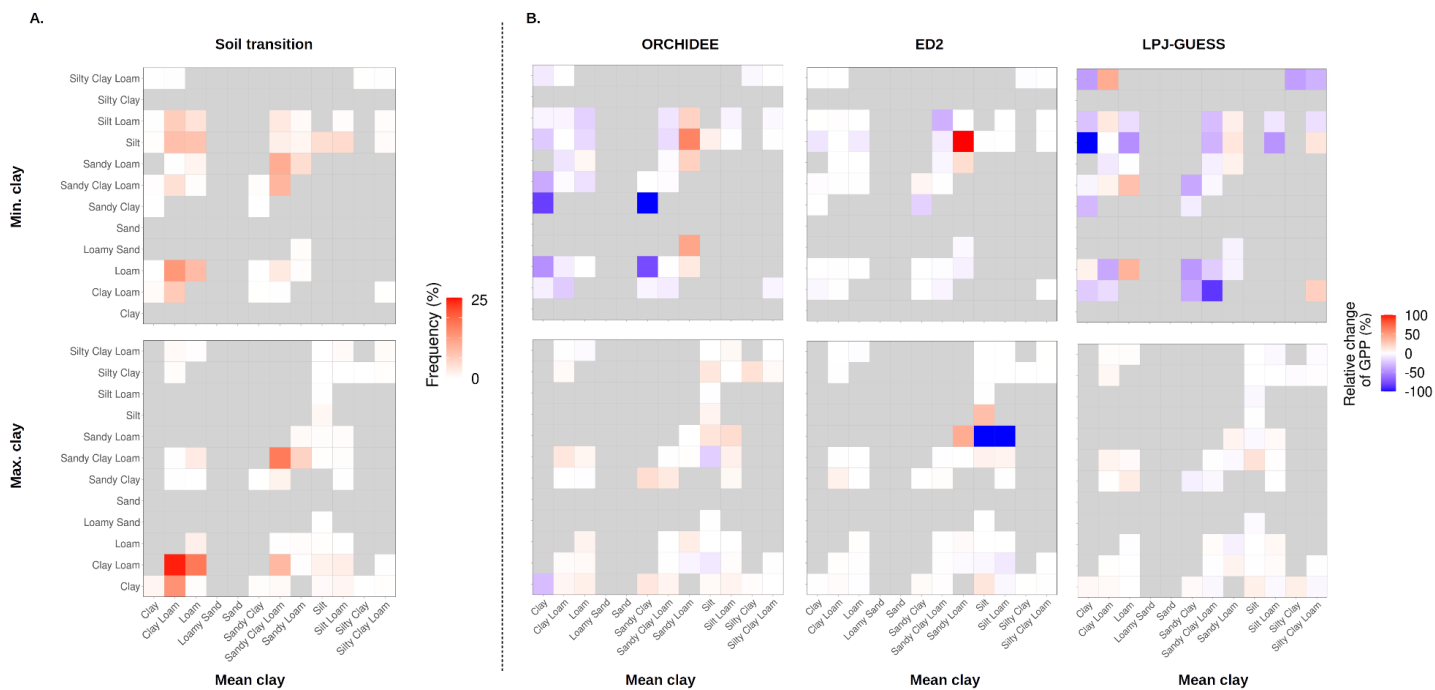


440 **Figure 3: Ecosystem GPP as a function of the soil drought stress index (SDI) as predicted at the end of the historical period (2016) by each terrestrial biosphere model used in this study. The SDI values range between 0 and 1, with no stress represented by SDI = 1, full stress conditions represented by SDI = 0 representing full stress. The boxplots represent the distributions of the stress index for each scenario and the coloured lines are the 95% quantile regression per scenario (with the same color legend). Each dot is a gridcell (1° resolution).**



445

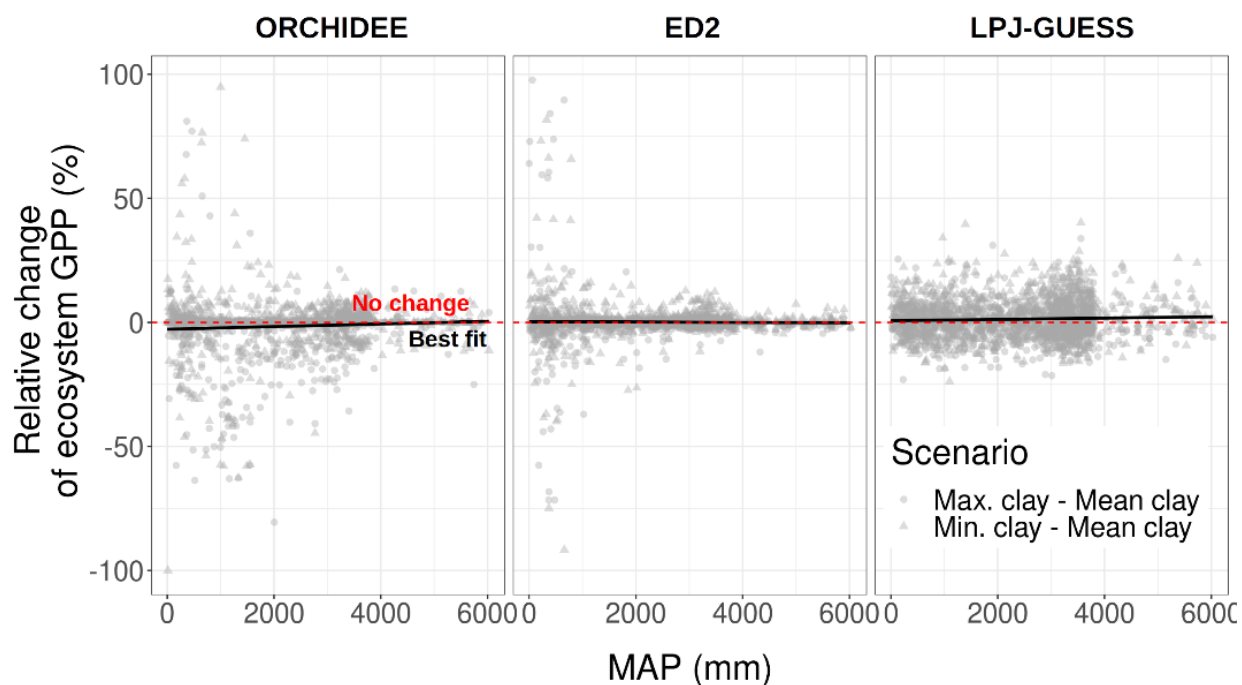
**Figure 4: Scenario (Max. clay: top row, and Min. clay: bottom row) vs reference (Mean clay scenario) GPP for each TBM used in this study. Each dot is the PFT-level GPP over a specific gridcell (1° resolution) at the end of the historical period (2016).**



450

**Figure 5: Soil transition matrix representing the frequencies of moving from one soil class to another when changing the soil textural map (A) and the relative change of ecosystem gross primary production (GPP) for each category of transition and terrestrial biosphere model (B) as predicted by each TBM at the end of the historical period. In A, the colour intensity represents the frequency of each transition. The grey cells are transitions that did not occur in the simulated scenarios.**





455

**Figure 6:** Relative change of the annual ecosystem GPP at the end of the historical simulation with the mean annual precipitation (MAP) for both scenarios (shapes) and all three TBMs considered in this study, across the entire simulated region (each point is a gridcell). The MAP is the annual average over the last ten years of the CRU-NCEP dataset forcing.



## References

- 460 Ahlström, A., G. Schurgers, A. Arneth, and B. Smith. 2012. “Robustness and Uncertainty in Terrestrial Ecosystem  
Carbon Response to CMIP5 Climate Change Projections.” *Environmental Research Letters* 7 (4): 044008.  
<https://doi.org/10.1088/1748-9326/7/4/044008>.
- Aragão, L. E. O. C., Y. Malhi, D. B. Metcalfe, J. E. Silva-Espejo, E. Jiménez, D. Navarrete, S. Almeida, et al. 2009.  
465 “Above- and below-Ground Net Primary Productivity across Ten Amazonian Forests on Contrasting Soils.”  
*Biogeosciences* 6 (12): 2759–78. <https://doi.org/10.5194/bg-6-2759-2009>.
- Avitabile, Valerio, Martin Herold, Gerard B. M. Heuvelink, Simon L. Lewis, Oliver L. Phillips, Gregory P. Asner,  
John Armston, et al. 2016. “An Integrated Pan-Tropical Biomass Map Using Multiple Reference Datasets.” *Global  
Change Biology* 22 (4): 1406–20. <https://doi.org/10.1111/gcb.13139>.
- 470 Baker, I. T., L. Prihodko, A. S. Denning, M. Goulden, S. Miller, and H. R. da Rocha. 2008. “Seasonal Drought  
Stress in the Amazon: Reconciling Models and Observations.” *Journal of Geophysical Research* 113 (G1):  
G00B01. <https://doi.org/10.1029/2007JG000644>.
- Barros, Alexandre Hugo Cezar, and Quirijn de Jong van Lier. 2014. “Pedotransfer Functions for Brazilian Soils.” In  
*Application of Soil Physics in Environmental Analyses: Measuring, Modelling and Data Integration*, edited by  
Wenceslau Gerales Teixeira, Marcos Bacis Ceddia, Marta Vasconcelos Ottoni, and Guilherme Kangussu  
475 Donnagema, 131–62. Progress in Soil Science. Cham: Springer International Publishing.  
[https://doi.org/10.1007/978-3-319-06013-2\\_6](https://doi.org/10.1007/978-3-319-06013-2_6).
- Batjes, N. H. 1997. “A World Dataset of Derived Soil Properties by FAO–UNESCO Soil Unit for Global  
Modelling.” *Soil Use and Management* 13 (1): 9–16. <https://doi.org/10.1111/j.1475-2743.1997.tb00550.x>.
- 480 Bonan, Gordon B. 2008. “Forests and Climate Change: Forcings, Feedbacks, and the Climate Benefits of Forests.”  
*Science* 320 (5882): 1444–49.
- Brienen, R J W, O L Phillips, T R Feldpausch, E Gloor, T R Baker, J Lloyd, G Lopez-Gonzalez, et al. 2015. “Long-  
Term Decline of the Amazon Carbon Sink.” *Nature* 519 (7543): 344–48. <https://doi.org/10.1038/nature14283>.
- Brooks, Royal Harvard, and Arthur Thomas Corey. 1964. *Hydraulic Properties of Porous Media*. Colorado State  
University.
- 485 Buckingham, Edgar, United States, Department of Agriculture, United States, and Bureau of Soils. 1907. *Studies on  
the Movement of Soil Moisture*. Washington,: Govt. Print. Off.
- Carminati, Andrea, and Mathieu Javaux. 2020. “Soil Rather Than Xylem Vulnerability Controls Stomatal Response  
to Drought.” *Trends in Plant Science* 25 (9): 868–80. <https://doi.org/10.1016/j.tplants.2020.04.003>.
- 490 Carsel, Robert F., and Rudolph S. Parrish. 1988. “Developing Joint Probability Distributions of Soil Water  
Retention Characteristics.” *Water Resources Research* 24 (5): 755–69. <https://doi.org/10.1029/WR024i005p00755>.
- Christoffersen, B. O., M. Gloor, S. Fauset, N. M. Fyllas, D. R. Galbraith, T. R. Baker, B. Kruijt, et al. 2016.  
“Linking Hydraulic Traits to Tropical Forest Function in a Size-Structured and Trait-Driven Model (TFS v.1-  
Hydro).” *Geosci. Model Dev.* 9 (11): 4227–55. <https://doi.org/10.5194/gmd-9-4227-2016>.
- 495 Clapp, R., and G. Hornberger. 1978. “Empirical Equations for Some Soil Hydraulic Properties.”  
<https://doi.org/10.1029/WR014I004P00601>.
- Collier, Nathan, Forrest M. Hoffman, David M. Lawrence, Gretchen Keppel-Aleks, Charles D. Koven, William J.  
Riley, Mingquan Mu, and James T. Randerson. 2018. “The International Land Model Benchmarking (ILAMB)  
System: Design, Theory, and Implementation.” *Journal of Advances in Modeling Earth Systems* 10 (11): 2731–54.  
<https://doi.org/10.1029/2018MS001354>.
- 500 Combe, Marie, Jordi Vilà-Guerau de Arellano, Huug G. Ouwensloot, and Wouter Peters. 2016. “Plant Water-Stress  
Parameterization Determines the Strength of Land–Atmosphere Coupling.” *Agricultural and Forest Meteorology*  
217 (February): 61–73. <https://doi.org/10.1016/j.agrformet.2015.11.006>.
- Condit, Richard, Bettina M. J. Engelbrecht, Delicia Pino, Rolando Pérez, and Benjamin L. Turner. 2013. “Species  
Distributions in Response to Individual Soil Nutrients and Seasonal Drought across a Community of Tropical  
505 Trees.” *Proceedings of the National Academy of Sciences* 110 (13): 5064–68.  
<https://doi.org/10.1073/pnas.1218042110>.
- Corlett, Richard T. 2016. “The Impacts of Droughts in Tropical Forests.” *Trends in Plant Science* 21 (7): 584–93.



<https://doi.org/10.1016/j.tplants.2016.02.003>.

Cosby, B. J., G. M. Hornberger, R. B. Clapp, and T. R. Ginn. 1984. “A Statistical Exploration of the Relationships of Soil Moisture Characteristics to the Physical Properties of Soils.” *Water Resources Research* 20 (6): 682–90. <https://doi.org/10.1029/WR020i006p00682>.

Darcy, Henry (1803-1858). n.d. “Les fontaines publiques de la ville de Dijon : exposition et application des principes à suivre et des formules à employer dans les questions de distribution d’eau... / par Henry Darcy,....” 659.

Doughty, Christopher E., D. B. Metcalfe, C. a. J. Girardin, F. Farfán Amézquita, D. Galiano Cabrera, W. Huaraca Huasco, J. E. Silva-Espejo, et al. 2015. “Drought Impact on Forest Carbon Dynamics and Fluxes in Amazonia.” *Nature* 519 (7541): 78–82. <https://doi.org/10.1038/nature14213>.

Duffy, Philip B., Paulo Brando, Gregory P. Asner, and Christopher B. Field. 2015. “Projections of Future Meteorological Drought and Wet Periods in the Amazon.” *Proceedings of the National Academy of Sciences* 112 (43): 13172–77. <https://doi.org/10.1073/pnas.1421010112>.

Eyring, Veronika, Sandrine Bony, Gerald A. Meehl, Catherine A. Senior, Bjorn Stevens, Ronald J. Stouffer, and Karl E. Taylor. 2016. “Overview of the Coupled Model Intercomparison Project Phase 6 (CMIP6) Experimental Design and Organization.” *Geoscientific Model Development* 9 (5): 1937–58. <https://doi.org/10.5194/gmd-9-1937-2016>.

Feldpausch, T. R., O. L. Phillips, R. J. W. Brienen, E. Gloor, J. Lloyd, G. Lopez-Gonzalez, A. Monteagudo-Mendoza, et al. 2016. “Amazon Forest Response to Repeated Droughts.” *Global Biogeochemical Cycles* 30 (7): 964–82. <https://doi.org/10.1002/2015GB005133>.

Fisher, Rosie A., and Charles D. Koven. 2020. “Perspectives on the Future of Land Surface Models and the Challenges of Representing Complex Terrestrial Systems.” *Journal of Advances in Modeling Earth Systems* 12 (4): e2018MS001453. <https://doi.org/10.1029/2018MS001453>.

Flack-Prain, Sophie, Patrick Meir, Yadvinder Malhi, Thomas L. Smallman, and Mathew Williams. 2021. “Does Economic Optimisation Explain LAI and Leaf Trait Distributions across an Amazon Soil Moisture Gradient?” *Global Change Biology* 27 (3): 587–605. <https://doi.org/10.1111/gcb.15368>.

Franklin, Oskar, Jacob Johansson, Roderick C. Dewar, Ulf Dieckmann, Ross E. McMurtrie, Åke Brännström, and Ray Dybzinski. 2012. “Modeling Carbon Allocation in Trees: A Search for Principles.” *Tree Physiology* 32 (6): 648–66. <https://doi.org/10.1093/treephys/tpr138>.

Friedlingstein, Pierre, Michael O’Sullivan, Matthew W. Jones, Robbie M. Andrew, Judith Hauck, Are Olsen, Glen P. Peters, et al. 2020. “Global Carbon Budget 2020.” *Earth System Science Data* 12 (4): 3269–3340. <https://doi.org/10.5194/essd-12-3269-2020>.

Fyllas, N. M., S. Patiño, T. R. Baker, G. Bielefeld Nardoto, L. A. Martinelli, C. A. Quesada, R. Paiva, et al. 2009. “Basin-Wide Variations in Foliar Properties of Amazonian Forest: Phylogeny, Soils and Climate.” *Biogeosciences* 6 (11): 2677–2708. <https://doi.org/10.5194/bg-6-2677-2009>.

Gatti, L. V., M. Gloor, J. B. Miller, C. E. Doughty, Y. Malhi, L. G. Domingues, L. S. Basso, et al. 2014. “Drought Sensitivity of Amazonian Carbon Balance Revealed by Atmospheric Measurements.” *Nature* 506 (7486): 76–80. <https://doi.org/10.1038/nature12957>.

Genuchten, M. Th. van. 1980. “A Closed-Form Equation for Predicting the Hydraulic Conductivity of Unsaturated Soils1.” *Soil Science Society of America Journal* 44 (5): 892. <https://doi.org/10.2136/sssaj1980.03615995004400050002x>.

Gerten, Dieter, Sibyll Schaphoff, Uwe Haberlandt, Wolfgang Lucht, and Stephen Sitch. 2004. “Terrestrial Vegetation and Water Balance—Hydrological Evaluation of a Dynamic Global Vegetation Model.” *Journal of Hydrology* 286 (1): 249–70. <https://doi.org/10.1016/j.jhydrol.2003.09.029>.

Green, J. K., J. Berry, P. Ciais, Y. Zhang, and P. Gentile. 2020. “Amazon Rainforest Photosynthesis Increases in Response to Atmospheric Dryness.” *Science Advances* 6 (47): eabb7232. <https://doi.org/10.1126/sciadv.abb7232>.

Harris, Philip P., Chris Huntingford, Peter M. Cox, John H. C. Gash, and Yadvinder Malhi. 2004. “Effect of Soil Moisture on Canopy Conductance of Amazonian Rainforest.” *Agricultural and Forest Meteorology* 3–4 (122): 215–27. <https://doi.org/10.1016/j.agrformet.2003.09.006>.

Hassink, J. 1992. “Effects of Soil Texture and Structure on Carbon and Nitrogen Mineralization in Grassland Soils.” *Biology and Fertility of Soils* 14 (2): 126–34. <https://doi.org/10.1007/BF00336262>.



- Haxeltine, A., and I. C. Prentice. 1996. “A General Model for the Light-Use Efficiency of Primary Production.” *Functional Ecology* 10 (5): 551–61. <https://doi.org/10.2307/2390165>.
- 560 Hengl, Tomislav, Jorge Mendes de Jesus, Gerard B. M. Heuvelink, Maria Ruiperez Gonzalez, Milan Kilibarda, Aleksandar Blagotić, Wei Shangguan, et al. 2017. “SoilGrids250m: Global Gridded Soil Information Based on Machine Learning.” *PLOS ONE* 12 (2): e0169748. <https://doi.org/10.1371/journal.pone.0169748>.
- Hodnett, Martin, and Javier Tomasella. 2002. “Marked Differences between van Genuchten Soil Water-Retention Parameters for Temperate and Tropical Soils: A New Water-Retention Pedo-Transfer Functions Developed for Tropical Soils.” *Geoderma* 108 (August): 155–80. [https://doi.org/10.1016/S0016-7061\(02\)00105-2](https://doi.org/10.1016/S0016-7061(02)00105-2).
- 565 Hubau, Wannes, Simon L. Lewis, Oliver L. Phillips, Kofi Affum-Baffoe, Hans Beeckman, Aida Cuní-Sanchez, Armandu K. Daniels, et al. 2020. “Asynchronous Carbon Sink Saturation in African and Amazonian Tropical Forests.” *Nature* 579 (7797): 80–87. <https://doi.org/10.1038/s41586-020-2035-0>.
- 570 Hurk, Bart van den, Hyungjun Kim, Gerhard Krinner, Sonia I. Seneviratne, Chris Derksen, Taikan Oki, Hervé Douville, et al. 2016. “LS3MIP (v1.0) Contribution to CMIP6: The Land Surface, Snow and Soil Moisture Model Intercomparison Project – Aims, Setup and Expected Outcome.” *Geoscientific Model Development* 9 (8): 2809–32. <https://doi.org/10.5194/gmd-9-2809-2016>.
- Jackson, R. B., J. Canadell, J. R. Ehleringer, H. A. Mooney, O. E. Sala, and E. D. Schulze. 1996. “A Global Analysis of Root Distributions for Terrestrial Biomes.” *Oecologia* 108 (3): 389–411. <https://doi.org/10.1007/BF00333714>.
- 575 Jiménez, Eliana M., María Cristina Peñuela-Mora, Carlos A. Sierra, Jon Lloyd, Oliver L. Phillips, Flavio H. Moreno, Diego Navarrete, et al. 2014. “Edaphic Controls on Ecosystem-Level Carbon Allocation in Two Contrasting Amazon Forests.” *Journal of Geophysical Research: Biogeosciences* 119 (9): 1820–30. <https://doi.org/10.1002/2014JG002653>.
- 580 Jirka, S, A J McDonald, M S Johnson, T R Feldpausch, E G Couto, and S J Riha. 2007. “Relationships between Soil Hydrology and Forest Structure and Composition in the Southern Brazilian Amazon.” *Journal of Vegetation Science* 18 (2): 183–94. <https://doi.org/10.1111/j.1654-1103.2007.tb02529.x>.
- 585 Joetzer, E., C. Delire, H. Douville, P. Ciais, B. Decharme, R. Fisher, B. Christoffersen, et al. 2014. “Predicting the Response of the Amazon Rainforest to Persistent Drought Conditions under Current and Future Climates: A Major Challenge for Global Land Surface Models.” *Geoscientific Model Development* 7 (6): 2933–50. <https://doi.org/10.5194/gmd-7-2933-2014>.
- Johnson, Michelle O., David Galbraith, Manuel Gloor, Hannes De Deurwaerder, Matthieu Guimberteau, Anja Rammig, Kirsten Thonicke, et al. 2016. “Variation in Stem Mortality Rates Determines Patterns of Above-Ground Biomass in Amazonian Forests: Implications for Dynamic Global Vegetation Models.” *Global Change Biology* 22 (12): 3996–4013. <https://doi.org/10.1111/gcb.13315>.
- 590 Kishné, A., Y. Yimam, C. Morgan, and B. Dornblaser. 2017. “Evaluation and Improvement of the Default Soil Hydraulic Parameters for the Noah Land Surface Model.” <https://doi.org/10.1016/J.GEODERMA.2016.09.022>.
- 595 Knox, R. G., M. Longo, A. L. S. Swann, K. Zhang, N. M. Levine, P. R. Moorcroft, and R. L. Bras. 2015. “Hydrometeorological Effects of Historical Land-Conversion in an Ecosystem-Atmosphere Model of Northern South America.” *Hydrology and Earth System Sciences* 19 (1): 241–73. <https://doi.org/10.5194/hess-19-241-2015>.
- 600 Krinner, G., Nicolas Viovy, Nathalie de Noblet-Ducoudré, Jérôme Ogée, Jan Polcher, Pierre Friedlingstein, Philippe Ciais, Stephen Sitch, and I. Colin Prentice. 2005. “A Dynamic Global Vegetation Model for Studies of the Coupled Atmosphere-Biosphere System.” *Global Biogeochemical Cycles* 19 (1). <https://doi.org/10.1029/2003GB002199>.
- 605 Laurance, William F, Philip M Fearnside, Susan G Laurance, Patricia Delamonica, Thomas E Lovejoy, Judy M Rankin-de Merona, Jeffrey Q Chambers, and Claude Gascon. 1999. “Relationship between Soils and Amazon Forest Biomass: A Landscape-Scale Study.” *Forest Ecology and Management* 118 (1): 127–38. [https://doi.org/10.1016/S0378-1127\(98\)00494-0](https://doi.org/10.1016/S0378-1127(98)00494-0).
- Li, Longhui, Ying-Ping Wang, Qiang Yu, Bernard Pak, Derek Eamus, Junhua Yan, Eva van Gorsel, and Ian T. Baker. 2012. “Improving the Responses of the Australian Community Land Surface Model (CABLE) to Seasonal Drought: IMPROVING CABLE IN RESPONSE TO DROUGHT.” *Journal of Geophysical Research: Biogeosciences* 117 (G4): n/a-n/a. <https://doi.org/10.1029/2012JG002038>.



- 610 Longo, Marcos, Ryan G. Knox, Naomi M. Levine, Luciana F. Alves, Damien Bonal, Plinio B. Camargo, David R. Fitzjarrald, et al. 2018. “Ecosystem Heterogeneity and Diversity Mitigate Amazon Forest Resilience to Frequent Extreme Droughts.” *New Phytologist* 219 (3): 914–31. <https://doi.org/10.1111/nph.15185>.
- Longo, Marcos, Ryan G. Knox, David M. Medvigy, Naomi M. Levine, Michael C. Dietze, Yeonjoo Kim, Abigail L. S. Swann, et al. 2019. “The Biophysics, Ecology, and Biogeochemistry of Functionally Diverse, Vertically and Horizontally Heterogeneous Ecosystems: The Ecosystem Demography Model, Version 2.2 – Part 1: Model Description.” *Geoscientific Model Development* 12 (10): 4309–46. <https://doi.org/10.5194/gmd-12-4309-2019>.
- 615 Lu, Jianrong, Qi Zhang, Adrian D. Werner, Yunliang Li, Sanyuan Jiang, and Zhiqiang Tan. 2020. “Root-Induced Changes of Soil Hydraulic Properties – A Review.” *Journal of Hydrology* 589 (October): 125203. <https://doi.org/10.1016/j.jhydrol.2020.125203>.
- Maeda, Eduardo Eiji, Hyungjun Kim, Luiz E. O. C. Aragão, James S. Famiglietti, and Taikan Oki. 2015. “Disruption of Hydroecological Equilibrium in Southwest Amazon Mediated by Drought.” *Geophysical Research Letters* 42 (18): 7546–53. <https://doi.org/10.1002/2015GL065252>.
- 620 Medeiros, João Carlos, Miguel Cooper, Jaqueline Dalla Rosa, Michel Grimaldi, and Yves Coquet. 2014. “Assessment of Pedotransfer Functions for Estimating Soil Water Retention Curves for the Amazon Region.” *Revista Brasileira de Ciência Do Solo* 38 (June): 730–43. <https://doi.org/10.1590/S0100-06832014000300005>.
- 625 Medvigy, D., S. C. Wofsy, J. W. Munger, D. Y. Hollinger, and P. R. Moorcroft. 2009. “Mechanistic Scaling of Ecosystem Function and Dynamics in Space and Time: Ecosystem Demography Model Version 2.” *Journal of Geophysical Research* 114 (G1). <https://doi.org/10.1029/2008JG000812>.
- Mencuccini, Maurizio, Stefano Manzoni, and Bradley Christoffersen. 2019. “Modelling Water Fluxes in Plants: From Tissues to Biosphere.” *New Phytologist* 222 (3): 1207–22. <https://doi.org/10.1111/nph.15681>.
- 630 Moeys, Julien. n.d. “The Soil Texture Wizard: R Functions for Plotting, Classifying, Transforming and Exploring Soil Texture Data,” 104.
- Mualem, Yechezkel. 1976. “A New Model for Predicting the Hydraulic Conductivity of Unsaturated Porous Media.” *Water Resources Research* 12 (3): 513–22. <https://doi.org/10.1029/WR012i003p00513>.
- Nachtergaele, F. O., H. van Velthuizen, L. Verelst, N. H. Batjes, J. A. Dijkshoorn, V. W. P. van Engelen, G. Fischer, et al. 2008. “Harmonized World Soil Database (Version 1.0).” <https://research.wur.nl/en/publications/harmonized-world-soil-database-version-10>.
- 635 Negrón Juárez, R. I., M. G. Hodnett, R. Fu, M. L. Gouden, and C. von Randow. 2007. “Control of Dry Season Evapotranspiration over the Amazonian Forest as Inferred from Observation at a Southern Amazon Forest Site.” *Journal of Climate* 20 (12): 2827–39. <https://doi.org/10.1175/JCLI4184.1>.
- 640 Neilson, Ronald P. 1995. “A Model for Predicting Continental-Scale Vegetation Distribution and Water Balance.” *Ecological Applications* 5 (2): 362–85. <https://doi.org/10.2307/1942028>.
- Nepstad, Daniel C., Ingrid Marisa Tohver, David Ray, Paulo Moutinho, and Georgina Cardinot. 2007. “Mortality of Large Trees and Lianas Following Experimental Drought in an Amazon Forest.” *Ecology* 88 (9): 2259–69. <https://doi.org/10.1890/06-1046.1>.
- 645 O’Connell, Christine S., Leilei Ruan, and Whendee L. Silver. 2018. “Drought Drives Rapid Shifts in Tropical Rainforest Soil Biogeochemistry and Greenhouse Gas Emissions.” *Nature Communications* 9 (1): 1348. <https://doi.org/10.1038/s41467-018-03352-3>.
- Orgeval, T. d’, J. Polcher, and P. de Rosnay. 2008. “Sensitivity of the West African Hydrological Cycle in ORCHIDEE to Infiltration Processes.” *Hydrology and Earth System Sciences* 12 (6): 1387–1401. <https://doi.org/10.5194/hess-12-1387-2008>.
- 650 Patil, Nitin Gorakh, and Surendra Kumar Singh. 2016. “Pedotransfer Functions for Estimating Soil Hydraulic Properties: A Review.” *Pedosphere* 26 (4): 417–30. [https://doi.org/10.1016/S1002-0160\(15\)60054-6](https://doi.org/10.1016/S1002-0160(15)60054-6).
- Peylin, P., J. Ghattas, P. Cadule, F. Cheruy, A. Ducharne, B. Guenet, J. Lathière, et al. In prep. “The Global Land Surface Model ORCHIDEE – Tag2.0.” <http://forge.ipsl.jussieu.fr/orchidee/browser/tags/ORCHIDEE20/ORCHIDEE/>.
- 655 Phillips, Oliver L., Luiz E. O. C. Aragão, Simon L. Lewis, Joshua B. Fisher, Jon Lloyd, Gabriela López-González, Yaduvinder Malhi, et al. 2009. “Drought Sensitivity of the Amazon Rainforest.” *Science* 323 (5919): 1344–47. <https://doi.org/10.1126/science.1164033>.



- 660 Plante, Alain F., Richard T. Conant, Catherine E. Stewart, Keith Paustian, and Johan Six. 2006. “Impact of Soil Texture on the Distribution of Soil Organic Matter in Physical and Chemical Fractions.” *Soil Science Society of America Journal* 70 (1): 287–96. <https://doi.org/10.2136/sssaj2004.0363>.
- Poggio, Laura, Luis M. de Sousa, Niels H. Batjes, Gerard B. M. Heuvelink, Bas Kempen, Eloi Ribeiro, and David Rossiter. 2021. “SoilGrids 2.0: Producing Soil Information for the Globe with Quantified Spatial Uncertainty.” *SOIL* 7 (1): 217–40. <https://doi.org/10.5194/soil-7-217-2021>.
- 665 Poulter, B., N. MacBean, A. Hartley, I. Khlystova, O. Arino, R. Betts, S. Bontemps, et al. 2015. “Plant Functional Type Classification for Earth System Models: Results from the European Space Agency’s Land Cover Climate Change Initiative.” *Geoscientific Model Development* 8 (7): 2315–28. <https://doi.org/10.5194/gmd-8-2315-2015>.
- Prentice, I. C., W. Cramer, S. P. Harrison, R. Leemans, R. A. Monserud, and A. M. Solomon. 1992. “A Global Biome Model Based on Plant Physiology and Dominance, Soil Properties and Climate.” *Journal of Biogeography* 19 (2): 117–34.
- 670 Prentice, I. Colin, Ning Dong, Sean M. Gleason, Vincent Maire, and Ian J. Wright. 2014. “Balancing the Costs of Carbon Gain and Water Transport: Testing a New Theoretical Framework for Plant Functional Ecology.” *Ecology Letters* 17 (1): 82–91. <https://doi.org/10.1111/ele.12211>.
- Qu, W., H. R. Bogen, J. A. Huisman, J. Vanderborght, M. Schuh, E. Priesack, and H. Vereecken. 2015. “Predicting Subgrid Variability of Soil Water Content from Basic Soil Information.” *Geophysical Research Letters* 42 (3): 789–96. <https://doi.org/10.1002/2014GL062496>.
- 675 Romano, Nunzio, and Alessandro Santini. 2002. “Water Retention and Storage: Field.” In , 721–38.
- Rosnay, P. de, and J. Polcher. 1998. “Modelling Root Water Uptake in a Complex Land Surface Scheme Coupled to a GCM.” *Hydrology and Earth System Sciences* 2 (2/3): 239–55. <https://doi.org/10.5194/hess-2-239-1998>.
- 680 Rosnay, P. de, J. Polcher, M. Bruen, and K. Laval. 2002. “Impact of a Physically Based Soil Water Flow and Soil-Plant Interaction Representation for Modeling Large-Scale Land Surface Processes.” *Journal of Geophysical Research (Atmospheres)* 107 (June): 4118. <https://doi.org/10.1029/2001JD000634>.
- Rowland, L., A. C. L. da Costa, D. R. Galbraith, R. S. Oliveira, O. J. Binks, A. a. R. Oliveira, A. M. Pullen, et al. 2015. “Death from Drought in Tropical Forests Is Triggered by Hydraulics Not Carbon Starvation.” *Nature* 528 (7580): 119–22. <https://doi.org/10.1038/nature15539>.
- 685 Running, Steve, Mu, Qiaozhen, and Zhao, Maosheng. 2015. “MOD17A2H MODIS/Terra Gross Primary Productivity 8-Day L4 Global 500m SIN Grid V006.” NASA EOSDIS Land Processes DAAC. <https://doi.org/10.5067/MODIS/MOD17A2H.006>.
- Silver, Whendee L., Jason Neff, Megan McGroddy, Ed Veldkamp, Michael Keller, and Raimundo Cosme. 2000. “Effects of Soil Texture on Belowground Carbon and Nutrient Storage in a Lowland Amazonian Forest Ecosystem.” *Ecosystems* 3 (2): 193–209. <https://doi.org/10.1007/s100210000019>.
- 690 Sitch, S., B. Smith, I. C. Prentice, A. Arneth, A. Bondeau, W. Cramer, J. O. Kaplan, et al. 2003. “Evaluation of Ecosystem Dynamics, Plant Geography and Terrestrial Carbon Cycling in the LPJ Dynamic Global Vegetation Model.” *Global Change Biology* 9 (2): 161–85. <https://doi.org/10.1046/j.1365-2486.2003.00569.x>.
- Smith, B., D. Wårlind, A. Arneth, T. Hickler, P. Leadley, J. Siltberg, and S. Zaehle. 2014. “Implications of Incorporating N Cycling and N Limitations on Primary Production in an Individual-Based Dynamic Vegetation Model.” *Biogeosciences* 11 (7): 2027–54. <https://doi.org/10.5194/bg-11-2027-2014>.
- 695 Smith, Benjamin, I. Colin Prentice, and Martin T. Sykes. 2001. “Representation of Vegetation Dynamics in the Modelling of Terrestrial Ecosystems: Comparing Two Contrasting Approaches within European Climate Space.” *Global Ecology and Biogeography* 10 (6): 621–37. <https://doi.org/10.1046/j.1466-822X.2001.t01-1-00256.x>.
- 700 “Soil Survey Manual (SSM) | NRCS Soils.” n.d. Accessed February 22, 2022. [https://www.nrcs.usda.gov/wps/portal/nrcs/detailfull/soils/ref/?cid=nrcs142p2\\_054262](https://www.nrcs.usda.gov/wps/portal/nrcs/detailfull/soils/ref/?cid=nrcs142p2_054262).
- Spinoni, Jonathan, Gustavo Naumann, Hugo Carrao, Paulo Barbosa, and Jürgen Vogt. 2014. “World Drought Frequency, Duration, and Severity for 1951–2010.” *International Journal of Climatology* 34 (8): 2792–2804. <https://doi.org/10.1002/joc.3875>.
- 705 Tafasca, Salma, Agnès Ducharne, and Christian Valentin. 2020. “Weak Sensitivity of the Terrestrial Water Budget to Global Soil Texture Maps in the ORCHIDEE Land Surface Model.” *Hydrology and Earth System Sciences* 24 (7): 3753–74. <https://doi.org/10.5194/hess-24-3753-2020>.



- 710 Telles, Everaldo de Carvalho Conceição, Plínio Barbosa de Camargo, Luiz A. Martinelli, Susan E. Trumbore, Enir Salazar da Costa, Joaquim Santos, Niro Higuchi, and Raimundo Cosme Oliveira Jr. 2003. “Influence of Soil Texture on Carbon Dynamics and Storage Potential in Tropical Forest Soils of Amazonia.” *Global Biogeochemical Cycles* 17 (2). <https://doi.org/10.1029/2002GB001953>.
- 715 Van Looy, Kris, Johan Bouma, Michael Herbst, John Koestel, Budiman Minasny, Umakant Mishra, Carsten Montzka, et al. 2017. “Pedotransfer Functions in Earth System Science: Challenges and Perspectives.” *Reviews of Geophysics* 55 (4): 1199–1256. <https://doi.org/10.1002/2017RG000581>.
- 720 Vanderborght, Jan, Valentin Couvreur, Felicien Meunier, Andrea Schnepf, Harry Vereecken, Martin Bouda, and Mathieu Javaux. 2021. “From Hydraulic Root Architecture Models to Macroscopic Representations of Root Hydraulics in Soil Water Flow and Land Surface Models.” *Hydrology and Earth System Sciences* 25 (9): 4835–60. <https://doi.org/10.5194/hess-25-4835-2021>.
- 725 Verbeeck, Hans, Philippe Peylin, Cédric Bacour, Damien Bonal, Kathy Steppe, and Philippe Ciais. 2011. “Seasonal Patterns of CO<sub>2</sub> Fluxes in Amazon Forests: Fusion of Eddy Covariance Data and the ORCHIDEE Model.” *Journal of Geophysical Research* 116 (G2). <https://doi.org/10.1029/2010jg001544>.
- Vereecken, Harry, Yakov Pachepsky, Heye Bogena, and Carsten Montzka. 2019. “Upscaling Issues in Ecohydrological Observations.” In *Observation and Measurement of Ecohydrological Processes*, edited by Xin Li and Harry Vereecken, 435–54. Ecohydrology. Berlin, Heidelberg: Springer. [https://doi.org/10.1007/978-3-662-48297-1\\_14](https://doi.org/10.1007/978-3-662-48297-1_14).
- 730 Viovy, Nicolas. 2018. “CRUNCEP Version 7 - Atmospheric Forcing Data for the Community Land Model.” UCAR/NCAR - Research Data Archive. <https://doi.org/10.5065/PZ8F-F017>.
- 735 Walko, Robert L., Larry E. Band, Jill Baron, Timothy G. F. Kittel, Richard Lammers, Tsengdar J. Lee, Dennis Ojima, et al. 2000. “Coupled Atmosphere–Biophysics–Hydrology Models for Environmental Modeling.” *Journal of Applied Meteorology* 39 (6): 931–44. [https://doi.org/10.1175/1520-0450\(2000\)039<0931:CABHMF>2.0.CO;2](https://doi.org/10.1175/1520-0450(2000)039<0931:CABHMF>2.0.CO;2).
- Xu, Xiangtao, David Medvigy, Jennifer S. Powers, Justin M. Becknell, and Kaiyu Guan. 2016. “Diversity in Plant Hydraulic Traits Explains Seasonal and Inter-Annual Variations of Vegetation Dynamics in Seasonally Dry Tropical Forests.” *New Phytologist* 212 (1): 80–95. <https://doi.org/10.1111/nph.14009>.
- 740 Yao, Yitong, Emilie Joetzer, Philippe Ciais, Nicolas Viovy, Fabio Cresto Aleina, Jerome Chave, Lawren Sack, et al. 2021. “Forest Fluxes and Mortality Response to Drought: Model Description (ORCHIDEE-CAN-NHA, R7236) and Evaluation at the Caxiuan&atilde; Drought Experiment.” *Geoscientific Model Development Discussions*, December, 1–38. <https://doi.org/10.5194/gmd-2021-362>.
- Zinn, Yuri L., Rattan Lal, Jerry M. Bigham, and Dimas V. S. Resck. 2007. “Edaphic Controls on Soil Organic Carbon Retention in the Brazilian Cerrado: Texture and Mineralogy.” *Soil Science Society of America Journal* 71 (4): 1204–14. <https://doi.org/10.2136/sssaj2006.0014>.